

Received April 18, 2019, accepted May 8, 2019, date of publication May 14, 2019, date of current version June 3, 2019.

Digital Object Identifier 10.1109/ACCESS.2019.2916548

Secure Transmission for Downlink NOMA Visible Light Communication Networks

CHUN DU¹, FAN ZHANG¹, SHUAI MA^{1,2}, YIXIAO TANG¹, HANG LI³, (Member, IEEE)
HONGMEI WANG¹, AND SHIYIN LI¹

¹School of Information and Control Engineering, China University of Mining and Technology, Xuzhou 221116, China

²State Key Laboratory of Integrated Services Networks, Xidian University, Xi'an 710071, China

³Shenzhen Research Institute of Big Data, Shenzhen 518172, China

Corresponding author: Shuai Ma (mashuai001@cumt.edu.cn)

The work of S. Ma and S. Li was supported in part by the National Natural Science Foundation of China under Grant 61701501 and Grant 61771474, in part by the Natural Science Foundation of Jiangsu Province under Grant BK20170287, in part by the China Postdoctoral Science Foundation under Grant 2016M600452, and in part by the Key Laboratory of Ocean Observation-Imaging Testbed of Zhejiang Province.

ABSTRACT In this paper, we consider the two key problems in the physical-layer security of nonorthogonal multiple access (NOMA) visible light communication (VLC) networks: investigating a closed-form achievable security rate and studying the optimal security beamforming design. Specifically, under the dimming control, practical power, and successive interference cancellation constraints, we derive both the outer and inner bounds of the security capacity region with closed-form expressions, which are evaluated via numerical results. Then, based on the proposed security-rate expression, we investigated the optimal security beamforming design to minimize the total LED power, and to maximize the minimum secrecy rate, respectively. Both the problems are nonconvex. We apply different relaxation techniques to efficiently solve them. The simulation results demonstrate the efficacy of the proposed security beamforming design schemes in the NOMA VLC networks.

INDEX TERMS NOMA, visible light communication, physical-layer secrecy, optimal beamforming.

I. INTRODUCTION

With the explosive increase of wireless data traffic, radio-frequency (RF) communications are suffering from congested spectrum bands and limited network capacity [1], [2]. Although the millimeter wave (mmWave) communication provides bandwidth from hundreds of megahertz to several gigahertz range, it is still unable to fully meet the demand in future wireless communications [3], [4]. Owing a broad license-free optical spectrum from 430 to 790 THz, visible light communication (VLC) is a promising complementary and even an alternative technology for the indoor next generation wireless networks [5]–[9]. With the deployed light emitting diode (LED), VLC simultaneously provides wireless communication and illumination, which enjoys several advantages, including high energy efficiency, high data rate, a large license-free bandwidth, no electromagnetic interference, being harmless for humans, and a low device cost.

The associate editor coordinating the review of this manuscript and approving it for publication was Miaowen Wen.

To better support multiple users and guarantee fairness of the multiuser VLC networks, nonorthogonal multiple access (NOMA) is a promising multiple access strategy [10]–[13]. By exploiting power-domain multiplexing, NOMA can support multiple users to access a network at the same time-frequency resources, for which the transmitter and receiver adopt superposition coding and successive interference cancellation (SIC), respectively [14]–[17]. Compared with orthogonal multiple access (OMA), NOMA significantly improves both the network capacity and user fairness, especially for high signal-to-noise ratio (SNR) scenarios [18]. Owing to the short transmission distance with a dominant line-of-sight (LOS) path, a high SNR scenario is common in VLC networks [19], which means that NOMA is well applicable for VLC networks.

One of major security issues in VLC is the passive eavesdropping in public areas, such as libraries, meeting rooms, and emporiums [20]. Unlike conventional encryption approaches in the upper layer, the physical-layer security ensures a secure transmission based on the differences between the received SNRs at the legitimate-user and

eavesdropper sides [21]–[24]. Moreover, as multiusers share the same time-frequency resources, the security of the physical layer is a necessity for enhancing the information security of NOMA VLC networks.

Recently, researchers [25]–[32] have paid some attentions to the physical-layer security of NOMA networks. Specifically, the secrecy-sum-rate-maximization problem was first investigated in [25] for a single-input single-output (SISO) NOMA network, which showed that the secrecy rate of the NOMA significantly outperforms that of the conventional OMA. Further, the secrecy-rate-maximization problems of NOMA networks have also been studied in the multiple-input-single-output (MISO) scenario [26] and multiple-input multiple-output (MIMO) scenario [28], where the central users are legitimate users and the cell-edge users are eavesdroppers. Tian *et al.* [27] investigated the MIMO-NOMA secrecy sum rate maximization problem under both the SIC and transmission-power constraints. By using stochastic geometry, Liu *et al.* [29] studied the physical-layer security of large-scale NOMA networks for both single- and multiple-antenna base-station scenarios, in which the eavesdropper exclusion area is proposed for improving the secrecy performance. In [33], a NOMA beamforming design was proposed to enhance the unicasting security performance and guarantee multicasting performance. He *et al.* [30] studied the transmission-power minimization problem with both the secrecy outage and quality-of-service (QoS) constraints, which showed the QoS secrecy tradeoff of NOMA scheme always outperforms that of the OMA scheme. By using the transmit-antenna-selection (TAS) strategies, the secrecy outage of two-user SISO and MISO NOMA systems was considered in [31]. Based on the classic Shannon capacity formula, the secrecy outage probability (SOP) was derived in [32] for NOMA VLC systems for both single and multiple eavesdropper scenarios.

Although the secrecy NOMA RF networks have been extensively investigated in [25]–[31], the research results cannot be directly applied to NOMA VLC networks. This could be explained from two perspectives [34]: the amplitude of VLC signals should be bounded considering human-eye safety; and by exploiting the intensity modulation and direct detection (IM/DD), the information of the VLC is denoted by the intensity of the light, which implies that in analysis, the transmitted signals are real and nonnegative. Therefore, the classic Shannon capacity formula with unbounded Gaussian input is inappropriate to quantify the secrecy rate of NOMA VLC networks. To the authors' best knowledge, neither the secrecy capacity nor the achievable secrecy rate of NOMA VLC networks is known, while these two are the key metrics for the physical-layer security of the NOMA VLC networks.

In this paper, we aim to derive the achievable security rate with closed-form, and further discuss optimal security beamforming design problems. Specifically, the main contributions are summarized as follows.

- By considering the dimming control, practical power constraints, and SIC constraints, we derive both the outer and inner bounds of the security capacity region with closed-form expressions for the NOMA VLC networks. To the best of our knowledge, the derived outer and inner bounds are the first theoretical bounds of the security capacity region in NOMA VLC networks. Moreover, the proposed inner bound represents the achievable security rate, which facilitates resource allocation and optimization to further improve the security of the NOMA network. Numerical results verify the tightness of the proposed outer and inner bounds.
- Based on the proposed achievable security-rate expression, we investigate the optimal beamforming design problems of the multiple-input single-output (MISO) NOMA VLC network. Specifically, we aimed to minimize the total LED power by using the dimming control while satisfying both user QoS requirements and secrecy-rate constraints. To solve this nonconvex problem, we propose a relaxation and restriction approach, in which the original nonconvex problem is first relaxed by utilizing the semidefinite relaxation (SDR) technique, and then approximated to a convex semidefinite program (SDP) by using a successive convex approximation (SCA) method. Thus, this problem can be efficiently solved by interior point methods.
- Furthermore, we investigated the secrecy rate maximization problem. More specifically, by considering both the dimming control and user QoS requirements, we propose the optimal beamforming design to maximize the minimum secrecy rate. However, this is a nonconvex programming problem, and by employing the relaxation and restriction approach, the nonconvex problem was reformulated to its quasi-convex form. Then, based on the bisection search algorithm, the quasi-convex problem was decomposed into a series of convex SDPs.

The rest of this paper is organized as follows. In Section II, we describe the NOMA VLC system model. In Section III, we derive both the outer and inner bounds of the secrecy capacity region of NOMA VLC networks. In Section IV, we investigate the optimal beamforming design to minimize the total LED power. Then, the optimal beamforming design to maximize the minimum secrecy rate is discussed in Section V. Next, simulations and an analysis to validate the proposed schemes are presented in Section VI, and Section VII concludes the paper.

II. NOMA VLC NETWORKS

Consider a multi-LED VLC network, which includes a light with N LEDs as the transmitter, K -photodiode (PD) legitimate users (Bobs), and a single PD eavesdropper (Eve), as shown in Fig. 1. During the downlink transmission, the VLC networks adopt the NOMA scheme. Let s_k denote the transmitted signal of Bob k , where $|s_k| \leq A_k$, $\mathbb{E}\{s_k\} = 0$, and $\mathbb{E}\{s_k^2\} = \varepsilon_k$. In addition, let $\mathbf{w}_k = [w_{k,1}, \dots, w_{k,N}]^T \in \mathbb{R}^N$

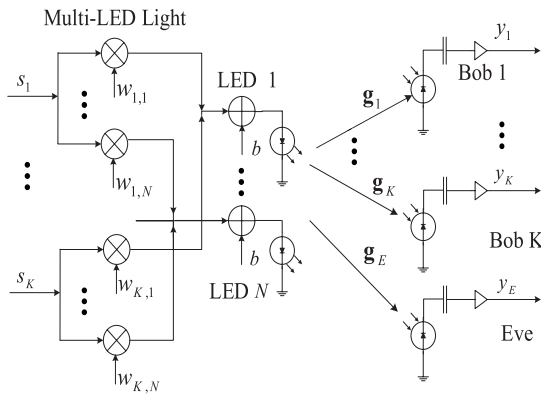


FIGURE 1. System of the NOMA VLC network.

denote the beamforming vector of the signal s_k . By adopting the superposition coding technique [35], the LEDs send the K signals $\{s_k\}$ to the Bobs, and the Eve intends to intercept the confidential information to the Bobs. Thus, the transmitted signal vector of the LEDs, i.e., $\mathbf{x} = [x_1, \dots, x_N]^T$ is given by

$$\mathbf{x} = \sum_{k=1}^K \mathbf{w}_k s_k + \mathbf{b}, \quad (1)$$

where $\mathbf{b} = [b, \dots, b]^T \in \mathbb{R}^N$ denotes the added direct-current vector to ensure the non-negativity of the transmitted signals, and $b \geq 0$. Moreover, the beamformer \mathbf{w}_k should be constrained by

$$\sum_{k=1}^K A_k |w_{k,n}| \leq b, \quad n \in \mathcal{N}, \quad (2)$$

where $\mathcal{N} \triangleq \{1, \dots, N\}$.

Thus, the transmitted power of LED light is

$$P_e = \mathbb{E} \left\{ \sum_{k=1}^K \|\mathbf{w}_k s_k\|^2 + \|\mathbf{b}\|^2 \right\} = \sum_{k=1}^K \varepsilon_k \|\mathbf{w}_k\|^2 + Nb^2. \quad (3)$$

Let P_o^{inst} and P_o^{ave} denote the instantaneous and average optical power of the LED lights, which are respectively given as

$$P_o^{inst} = \sum_{k=1}^K \sum_{n=1}^N w_{k,n} s_k + Nb, \quad (4a)$$

$$P_o^{ave} = \mathbb{E} (P_o^{inst}) = Nb. \quad (4b)$$

Moreover, VLC networks should satisfy both eye safety and practical illumination constraints by the dimming control [34], [36]. Specifically, the beamformer \mathbf{w}_k should also satisfy

$$\sum_{k=1}^K A_k \mathbf{w}_k^T \mathbf{e}_n + b \leq I_H, \quad \forall n \in \mathcal{N}, \quad (5)$$

where I_H is the maximum current of the LED. The dimming level τ is defined as the ratio of the average optical power P_o^{ave} to the maximum optical power P_T as follows

$$\tau = \frac{P_o^{ave}}{P_T} = \frac{Nb}{P_T}, \quad (6)$$

where $0 < \tau \leq 1$.

At the receiver side, the light signals are received from not only the line-of-sight (LOS) path but also the paths of reflections caused by the reflection on the ceiling, floor, and walls [37]. Fath and Haas [19] and Wang *et al.* [38] showed that the power of the LOS path is significantly higher than that of the reflection paths. Therefore, only the LOS path is adopted in this paper. Let $g_{k,n}$ denote the gain of the LOS path from the n th LED to Bob k , which can be expressed as [37]

$$g_{k,n} = \begin{cases} \frac{(m+1)A_R}{2\pi d_{k,n}^2} \cos^m(\phi_n) \cos(\psi_k), & \text{if } |\psi_k| \leq \psi_{FOV}; \\ 0, & \text{otherwise,} \end{cases} \quad (7)$$

where m denotes the Lambertian emission order; A_R is the receiver area; $d_{k,n}$ is the distance from the n th LED and Bob k ; ϕ_n is the angle of irradiance of the n th LED; ψ_k is the angle of incidence of Bob k ; and ψ_{FOV} denotes the field-of-view (FOV) of the receiver.

Analogously, the gain of LOS path between the n th LED and Eve $g_{E,n}$ is defined similar to (7).

Hence, the received signals by Bob k and Eve are respectively given by

$$y_k = \sum_{j=1}^K \mathbf{g}_k^T \mathbf{w}_j s_j + \mathbf{g}_k^T \mathbf{b} + n_k, \quad 1 \leq k \leq K, \quad (8a)$$

$$y_E = \sum_{j=1}^K \mathbf{g}_E^T \mathbf{w}_j s_j + \mathbf{g}_E^T \mathbf{b} + n_E, \quad (8b)$$

where $\mathbf{g}_k \triangleq [g_{k,1}, \dots, g_{k,N}]^T$ denotes the channel vector between the light and Bob k , $\mathbf{g}_E \triangleq [g_{E,1}, \dots, g_{E,N}]^T$ denotes the channel vector between the light and Eve, n_k denotes the received Gaussian noise at Bob k with zero mean and variance σ_k^2 , and n_E denotes the received Gaussian noise at Eve's end with zero mean and variance σ_k^2 .

Assume that the norm of the channel vectors $\left\{ \left\| \mathbf{g}_k^T \varepsilon_k^{1/2} \right\| \right\}_{k=1}^K$ follows $\left\| \mathbf{g}_1^T \varepsilon_1^{1/2} \right\| \leq \left\| \mathbf{g}_2^T \varepsilon_2^{1/2} \right\| \leq \dots \leq \left\| \mathbf{g}_K^T \varepsilon_K^{1/2} \right\|$. By employing the SIC, Bob k can decode and delete the interferences $\{s_i\}_{i=1}^{k-1}$, while $\{s_i\}_{i=k+1}^K$ cannot be removed. Thus, after SIC, the residual signal of the Bob is

$$y_{k,i}^{SIC} = \sum_{j=i}^K \mathbf{g}_k^T \mathbf{w}_j s_j + \mathbf{g}_k^T \mathbf{b} + n_k, \quad 1 \leq i \leq k \leq K. \quad (9)$$

III. SECURITY CAPACITY REGION OF NOMA NETWORKS

So far, the secrecy capacity region of the NOMA VLC network is an open problem. Let R_i^{sec} denote the secrecy capacity

of s_i in NOMA VLC network such that [20], [24], [39]

$$R_i^{\text{sec}} = \max_{\{p_i(s_i)\}} \left[\min_{k \in K} I(s_i; y_{k,i}^{\text{SIC}}) - I(s_i; y_E) \right]^+ \quad (10)$$

where $p_i(s_i)$ is the distribution of s_i . Unfortunately, the corresponding optimization problem (10) is difficult to solve explicitly under the amplitude constraint. Owing to the amplitude constraint, the secrecy capacity of NOMA VLC networks achieving distribution $p_i(s_i)$ is discrete [40]. However, both the secrecy capacity and the corresponding discrete distribution can only be approached via numerical calculation, without closed form expressions. To overcome the challenge, we developed both upper and lower bounds of the secrecy capacity with closed form expressions for the NOMA VLC network.

A. OUTER BOUND

Let $R_{k,i}^U$ denote the upper bound of $I(s_i; y_{k,i}^{\text{SIC}})$, i.e., the upper bound of the rate of decoding message s_i by Bob k , where $1 \leq i \leq k \leq K$. Moreover, let $R_{E,i}^L$ denote the lower bound of $I(s_i; y_E)$, i.e., the lower bound of the rate of decoding message s_i by Eve. According to the results in [41] and [42], $R_{k,i}^U$ and $R_{E,i}^L$ are respectively given by

$$R_{k,i}^U = \frac{1}{2} \log_2 \frac{2\pi\sigma_k^2 + 2\pi \sum_{j=i}^K |\mathbf{g}_k^T \mathbf{w}_j|^2 \varepsilon_j}{2\pi\sigma_k^2 + \Gamma_{k,i} \sum_{m=i+1}^K |\mathbf{g}_k^T \mathbf{w}_m|^2 e^{1+2(\alpha_m + \gamma_m \varepsilon_m)}}, \quad (11a)$$

$$R_{E,i}^L = \frac{1}{2} \log_2 \frac{2\pi\sigma_E^2 + \sum_{n=1}^K |\mathbf{g}_E^T \mathbf{w}_n|^2 e^{1+2(\alpha_n + \gamma_n \varepsilon_n)}}{2\pi\sigma_E^2 + 2\pi \sum_{l=1, l \neq i}^K |\mathbf{g}_E^T \mathbf{w}_l|^2 \varepsilon_l}, \quad (11b)$$

where α_j , β_j , and γ_j can be obtained by solving the equations

$$T_j(A_j) - T_j(-A_j) = e^{1+\alpha_j}, \quad (12a)$$

$$\beta_j \left(e^{A_j(\beta_j - \gamma_j A_j)} - e^{1+\alpha_j} - e^{-A_j(\beta_j + \gamma_j A_j)} \right) = 0, \quad (12b)$$

$$e^{A_j(\beta_j - \gamma_j A_j)} \left((\beta_j - 2\gamma_j A_j) e^{-2A_j \beta_j} - \beta_j - 2\gamma_j A_j \right) + (\beta_j^2 + 2\gamma_j) e^{1+\alpha_j} = 4\gamma_j^2 \varepsilon_j e^{1+\alpha_j}, \quad (12c)$$

and $T_j(X) = \sqrt{\pi} \frac{e^{\frac{\beta_j^2}{4\gamma_j}} \operatorname{erf}\left(\frac{\beta_j + 2\gamma_j X}{2\sqrt{\gamma_j}}\right)}{2\sqrt{\gamma_j}}$, $\Gamma_{k,i}$ is an indicator function, which can be given as follows:

$$\Gamma_{k,i} \triangleq \begin{cases} 1, & \forall (k, i) \neq (K, K) \\ 0, & \forall (k, i) = (K, K). \end{cases} \quad (13)$$

Then, the upper bound of secrecy capacity R_i^{sec} is given by

$$R_i^{\text{sec}} \leq \min_{k \in K} \left[R_{k,i}^U - R_{E,i}^L \right]^+. \quad (14)$$

Let $\mathcal{R}_{outer}^{\text{sec}}$ denote the secrecy channel capacity region of NOMA VLC networks bounded by (11), which is given by

$$\mathcal{R}_{outer}^{\text{sec}} \triangleq \left\{ r_1^{\text{sec}}, \dots, r_K^{\text{sec}} \mid r_i^{\text{sec}} \in \mathbb{R}^+, r_i^{\text{sec}} \leq \left[\min_{k \in K} R_{k,i}^U - R_{E,i}^L \right]^+, i = 1, \dots, K \right\}. \quad (15)$$

B. INNER BOUND

Let $R_{k,i}^L$ denote the lower bound of $I(s_i; y_{k,i}^{\text{SIC}})$, i.e., the lower bound of the rate of decoding message s_i by Bob k , where $1 \leq i \leq k \leq K$. Moreover, let $R_{E,i}^U$ denote the upper bound of $I(s_i; y_E)$, i.e., the upper bound of the rate of decoding message s_i by Eve. Based on the results in [41] and [42], $R_{k,i}^L$ and $R_{E,i}^U$ are respectively given by

$$R_{k,i}^L = \frac{1}{2} \log_2 \frac{2\pi\sigma_k^2 + \sum_{j=i}^K |\mathbf{g}_k^T \mathbf{w}_j|^2 e^{1+2(\alpha_j + \gamma_j \varepsilon_j)}}{2\pi\sigma_k^2 + 2\pi \Gamma_{k,i} \sum_{m=i+1}^K |\mathbf{g}_k^T \mathbf{w}_m|^2 \varepsilon_m}, \quad (16a)$$

$$R_{E,i}^U = \frac{1}{2} \log_2 \frac{2\pi\sigma_E^2 + 2\pi \sum_{n=1}^K |\mathbf{g}_E^T \mathbf{w}_n|^2 \varepsilon_n}{2\pi\sigma_E^2 + \sum_{l=1, l \neq i}^K |\mathbf{g}_E^T \mathbf{w}_l|^2 e^{1+2(\alpha_l + \gamma_l \varepsilon_l)}}. \quad (16b)$$

Then, the lower bound of secrecy capacity C_i^{sec} is given by

$$R_i^{\text{sec}} \geq \min_{k \in K} \left[R_{k,i}^L - R_{E,i}^U \right]^+. \quad (17)$$

Let $\mathcal{R}_{inner}^{\text{sec}}$ denote the achievable secrecy-rate region of NOMA VLC networks bounded by (16), which is given by

$$\mathcal{R}_{inner}^{\text{sec}} \triangleq \left\{ r_1^{\text{sec}}, \dots, r_K^{\text{sec}} \mid r_i^{\text{sec}} \in \mathbb{R}^+, r_i^{\text{sec}} \geq \left[\min_{k \in K} R_{k,i}^L - R_{E,i}^U \right]^+, i = 1, \dots, K \right\}. \quad (18)$$

IV. OPTIMAL SECURITY BEAMFORMING DESIGN FOR NOMA VLC NETWORKS

With explicit closed-form achievable security rate expression, we propose the optimal secrecy beamforming design for total transmission power minimization problem and minimum secrecy rate maximization problem for the MISO NOMA VLC network.

A. TOTAL TRANSMIT POWER MINIMIZATION

In this subsection, we seek to minimize the total transmit power while satisfying the QoS requirements of the Bobs, secrecy-rate constraints, and LED-power constraints. Mathematically, the transmit power minimization problem of the MISO NOMA VLC network can be formulated as:

$$\min_{\{\mathbf{w}_k\}_{k=1}^K} \sum_{k=1}^K \varepsilon_k \|\mathbf{w}_k\|^2 \quad (19a)$$

$$s.t. R_{k,i} \geq r_i, \quad 1 \leq i \leq k \leq K, \quad (19b)$$

$$\min_{k \in K} \left[R_{k,i}^L - R_{E,i}^U \right]^+ \geq r_i^{\text{sec}}, \quad 1 \leq i \leq k \leq K, \quad (19c)$$

$$\sum_{k=1}^K A_k \mathbf{w}_k^T \mathbf{e}_n \leq \min \{b, I_H - b\}, \quad \forall n \in \mathcal{N}, \quad (19d)$$

where r_i is the QoS requirement of decoding message s_i , R_i is the minimum secrecy rate of message s_i , and $\min \{b, I_H - b\}$ denotes the combination of per-LED power constraints and dimming control. Owing to constraints (19b) and (19c), optimization problem (19) is nonconvex and difficult to solve.

To overcome the nonconvex difficulty, we first introduce auxiliary variables as follows:

$$\hat{\mathbf{w}} \triangleq [\mathbf{w}_1^T, \dots, \mathbf{w}_K^T]^T, \quad (20a)$$

$$\hat{\mathbf{d}} \triangleq [\varepsilon_1^{1/2}, \dots, \varepsilon_K^{1/2}]^T \otimes \mathbf{1}_N, \quad (20b)$$

$$\mathbf{G}_{k,i} \triangleq \text{diag} \{0, \dots, 0, e^{1+2(\alpha_i + \gamma_i \varepsilon_i)}, \dots, e^{1+2(\alpha_K + \gamma_K \varepsilon_K)}\} \otimes \mathbf{g}_k \mathbf{g}_k^T, \quad (20c)$$

$$\bar{\mathbf{G}}_{k,i} \triangleq 2\pi \Gamma_{k,i} \text{diag} \{0, l, \dots, 0, \varepsilon_{i+1}, \dots, \varepsilon_K\} \otimes \mathbf{g}_k \mathbf{g}_k^T, \quad (20d)$$

$$\mathbf{D}_i \triangleq 2\pi \text{diag} \{\varepsilon_1, \dots, \varepsilon_K\} \otimes \mathbf{g}_E \mathbf{g}_E^T, \quad (20e)$$

$$\bar{\mathbf{D}}_i \triangleq \text{diag} \left\{ e^{1+2(\alpha_i + \gamma_i \varepsilon_i)}, \dots, e^{1+2(\alpha_{i-1} + \gamma_{i-1} \varepsilon_{i-1})}, 0, e^{1+2(\alpha_{i+1} + \gamma_{i+1} \varepsilon_{i+1})}, \dots, e^{1+2(\alpha_K + \gamma_K \varepsilon_K)} \right\} \otimes \mathbf{g}_E \mathbf{g}_E^T, \quad (20f)$$

$$\mathbf{a}_n \triangleq [A_1, \dots, A_K]^T \otimes \mathbf{e}_n, \quad (20g)$$

$$c_{k,i} \triangleq (2^{2r_i} - 1) 2\pi \sigma_k^2, \quad (20h)$$

where $\mathbf{1}_N$ is a $N \times 1$ vector with all elements equal to 1 and \mathbf{e}_i is a unit vector with the i th element equal to 1. Based on the auxiliary variables in (20), problem (19) can be equivalently reformulated as follows:

$$\min_{\hat{\mathbf{w}}} \|\hat{\mathbf{w}} \odot \hat{\mathbf{d}}\|^2 \quad (21a)$$

$$s.t. \hat{\mathbf{w}}^T \left((\mathbf{G}_{k,i} - 2^{2r_i} \bar{\mathbf{G}}_{k,i}) \right) \hat{\mathbf{w}} \geq c_{k,i}, \quad 1 \leq i \leq k \leq K, \quad (21b)$$

$$\frac{1}{2} \log_2 \left(\frac{2\pi \sigma_k^2 + \hat{\mathbf{w}}^T \mathbf{G}_{k,i} \hat{\mathbf{w}}}{2\pi \sigma_k^2 + \hat{\mathbf{w}}^T \bar{\mathbf{G}}_{k,i} \hat{\mathbf{w}}} \right) \left(\frac{2\pi \sigma_E^2 + \hat{\mathbf{w}}^T \mathbf{D}_i \hat{\mathbf{w}}}{2\pi \sigma_E^2 + \hat{\mathbf{w}}^T \bar{\mathbf{D}}_i \hat{\mathbf{w}}} \right) \geq r_i^{\text{sec}}, \quad 1 \leq i \leq K, \quad (21c)$$

$$\hat{\mathbf{w}}^T \mathbf{a}_n \mathbf{a}_n^T \hat{\mathbf{w}} \leq \min \{b^2, (I_H - b)^2\}, \quad \forall n \in \mathcal{N}. \quad (21d)$$

Problem (21) is a quadratically constrained quadratic problem, and in general is NP-hard.

Then, we adopted the SDR technique to handle the nonconvex constraints in (21). Specifically, by applying

$$\mathbf{W} = \hat{\mathbf{w}} \hat{\mathbf{w}}^T \Leftrightarrow \mathbf{W} \succeq \mathbf{0}, \quad \text{rank}(\mathbf{W}) = 1, \quad (22)$$

and dropping nonconvex constraint $\text{rank}(\mathbf{W}) = 1$, problem (21) can be relaxed as follows:

$$\min_{\mathbf{W}} \text{Tr} \left(\mathbf{W} \odot (\hat{\mathbf{d}} \hat{\mathbf{d}}^T) \right) \quad (23a)$$

$$s.t. \text{Tr} \left(\mathbf{W} \left(\mathbf{G}_{k,i} - 2^{2r_i} \bar{\mathbf{G}}_{k,i} \right) \right) \geq c_{k,i}, \quad 1 \leq i \leq k \leq K, \quad (23b)$$

$$\frac{2^{2r_i^{\text{sec}}} (2\pi \sigma_k^2 + \text{Tr}(\mathbf{W} \bar{\mathbf{G}}_{k,i})) (2\pi \sigma_E^2 + \text{Tr}(\mathbf{W} \mathbf{D}_i))}{(2\pi \sigma_k^2 + \text{Tr}(\mathbf{W} \mathbf{G}_{k,i})) (2\pi \sigma_E^2 + \text{Tr}(\mathbf{W} \bar{\mathbf{D}}_i))} \leq 1, \quad 1 \leq i \leq k \leq K, \quad (23c)$$

$$\text{Tr} \left(\mathbf{W} \mathbf{a}_n \mathbf{a}_n^T \right) \leq \min \{b^2, (I_H - b)^2\}, \quad \forall n \in \mathcal{N}, \quad (23d)$$

$$\mathbf{W} \succeq \mathbf{0}. \quad (23e)$$

So far, problem (23) is still nonconvex owing to constraint (23b). In the following, we adopt the restrictive step to convert problem (23) to its corresponding convex form. Specifically, we first introduce the following exponential terms:

$$e^{x_{k,i}} \triangleq 2\pi \sigma_k^2 + \text{Tr}(\mathbf{W} \mathbf{G}_{k,i}), \quad (24a)$$

$$e^{x_i} \triangleq 2\pi \sigma_E^2 + \text{Tr}(\mathbf{W} \bar{\mathbf{D}}_i), \quad (24b)$$

$$e^{y_{k,i}} \triangleq 2\pi \sigma_k^2 + \text{Tr}(\mathbf{W} \bar{\mathbf{G}}_{k,i}), \quad (24c)$$

$$e^{y_i} \triangleq 2\pi \sigma_E^2 + \text{Tr}(\mathbf{W} \mathbf{D}_i), \quad (24d)$$

where $x_{k,i}$, x_i , $y_{k,i}$, and y_i are slack variables, and $1 \leq i \leq k \leq K$. Then, based on the introduced variables (24), problem (23) can be restricted as follows:

$$\min_{\mathbf{W}, \{x_{k,i}\}, \{x_i\}, \{y_{k,i}\}, \{y_i\}} \text{Tr} \left(\mathbf{W} \odot (\hat{\mathbf{d}} \hat{\mathbf{d}}^T) \right) \quad (25a)$$

$$s.t. 2^{2r_i^{\text{sec}}} e^{y_{k,i} + y_i - x_{k,i} - x_i} \leq 1, \quad 1 \leq i \leq k \leq K, \quad (25b)$$

$$e^{x_{k,i}} \leq 2\pi \sigma_k^2 + \text{Tr}(\mathbf{W} \mathbf{G}_{k,i}), \quad 1 \leq i \leq k \leq K, \quad (25c)$$

$$e^{x_i} \leq 2\pi \sigma_E^2 + \text{Tr}(\mathbf{W} \bar{\mathbf{D}}_i), \quad 1 \leq i \leq K, \quad (25d)$$

$$e^{y_{k,i}} \geq 2\pi \sigma_k^2 + \text{Tr}(\mathbf{W} \bar{\mathbf{G}}_{k,i}), \quad 1 \leq i \leq k \leq K, \quad (25e)$$

$$e^{y_i} \geq 2\pi \sigma_E^2 + \text{Tr}(\mathbf{W} \mathbf{D}_i), \quad 1 \leq i \leq K, \quad (25f)$$

Note that constraints (26b), (25c), and (25d) are convex, while constraints (25e) and (25f) are still nonconvex. Based on the Taylor series expansion of $a^{\hat{x}} + (x - \hat{x}) a^{\hat{x}} \ln a \leq a^x$, both constraints (25e) and (25f) can be respectively linearized as follows:

$$2\pi \sigma_k^2 + \text{Tr}(\mathbf{W} \bar{\mathbf{G}}_{k,i}) \leq e^{\hat{y}_{k,i}} (y_{k,i} - \hat{y}_{k,i} + 1), \quad (26a)$$

$$2\pi \sigma_E^2 + \text{Tr}(\mathbf{W} \mathbf{D}_i) \leq e^{\hat{y}_i} (y_i - \hat{y}_i + 1), \quad (26b)$$

where $\hat{y}_{k,i}$ and \hat{y}_i are feasible points of problem (25).

Thus, problem (25) can be restrictedly approximated to its convex form as:

$$\min_{\mathbf{W}, \{x_{k,i}\}, \{x_i\}, \{y_{k,i}\}, \{y_i\}} \text{Tr} \left(\mathbf{W} \odot (\hat{\mathbf{d}} \hat{\mathbf{d}}^T) \right) \quad (26a), (26b), (25c), (25d), (25e), (25f)$$

$$(23b), (23d), (23e). \quad (27)$$

With the given $\hat{y}_{k,i}$ and \hat{y}_i , problem (27) is convex, and can be efficiently solved using standard convex solvers [43]. Then, $(\hat{y}_{k,i}, \hat{y}_i)$ are updated by optimal solution $(y_{k,i}, y_i)$ of (27), and problem (27) is iteratively solved until it converges. As shown in [44], the SCA method can converge to a stable point. Let \mathbf{W}^* denote the optimal solution of problem (27). If $\text{rank}(\mathbf{W}^*) = 1$, the optimal beamforming vectors of problem (19) can be obtained through eigenvalue decomposition. However, owing to SDR, the rank of matrix \mathbf{W}^* may be higher than 1, and the Gaussian randomization procedure can then be used to generate a high-quality feasible beamformer vector of problem (19).

B. MINIMUM SECRECY RATE MAXIMIZATION

Given the QoS requirements of Bob, the dimming control and pre-LED power constraints, our goal is to optimize the beamforming design such that the minimum secrecy rate of the NOMA VLC network is maximized. To this end, we consider the following beamforming design problem for the minimum secrecy rate maximization

$$\max_{\{\mathbf{w}_i\}} \min_{k,i} [R_{k,i}^L - R_{E,i}^U]^+ \quad (28a)$$

$$s.t. R_{k,i} \geq r_i, \quad 1 \leq i \leq k \leq K, \quad (28b)$$

$$\sum_{k=1}^K \varepsilon_k \|\mathbf{w}_k\|^2 \leq P_{total}, \quad (28c)$$

$$\sum_{k=1}^K A_k |w_{k,n}| \leq \min\{b, (I_H - b)\}, \quad \forall n \in \mathcal{N}, \quad (28d)$$

where P_{total} is the maximum total transmitting power. Problem (28) is nonconvex and intractable.

In the following, we first apply the relaxation step to problem (29). Specifically, by introducing slack variable r_s and $\mathbf{W} = \hat{\mathbf{w}}\hat{\mathbf{w}}^T$ and by adopting the SDR technique, problem (29) can be reformulated as follows:

$$\max_{\mathbf{W}, r_s} r_s \quad (29a)$$

$$s.t. \frac{2^{2r_s} (2\pi\sigma_k^2 + \text{Tr}(\mathbf{W}\bar{\mathbf{G}}_{k,i})) (2\pi\sigma_E^2 + \text{Tr}(\mathbf{W}\mathbf{D}_i))}{(2\pi\sigma_k^2 + \text{Tr}(\mathbf{W}\mathbf{G}_{k,i})) (2\pi\sigma_E^2 + \text{Tr}(\mathbf{W}\bar{\mathbf{D}}_i))} \leq 1, \quad (29b)$$

$$1 \leq i \leq k \leq K, \quad (29b)$$

$$\text{Tr}(\mathbf{W}(\mathbf{G}_{k,i} - 2^{2r_i}\bar{\mathbf{G}}_{k,i})) \geq c_{k,i}, \quad 1 \leq i \leq k \leq K, \quad (29c)$$

$$\text{Tr}(\mathbf{W} \odot (\hat{\mathbf{d}}\hat{\mathbf{d}}^T)) \leq P_{total}, \quad (29d)$$

$$\text{Tr}(\mathbf{W}\mathbf{a}_n\mathbf{a}_n^T) \leq \min\{b^2, (I_H - b)^2\}, \quad \forall n \in \mathcal{N}, \quad (29e)$$

$$\mathbf{W} \succeq \mathbf{0}. \quad (29f)$$

Owing to the nonconvex constraint of (29b), problem (29) is still nonconvex. In the following, we adopt the restriction step, and define the slack variables as follows:

$$2\pi\sigma_k^2 + \text{Tr}(\mathbf{W}\mathbf{G}_{k,i}) \geq e^{y_{k,i}}, \quad 1 \leq i \leq k \leq K, \quad (30a)$$

$$2\pi\sigma_E^2 + \text{Tr}(\mathbf{W}\bar{\mathbf{D}}_i) \geq e^{x_i}, \quad 1 \leq i \leq K, \quad (30b)$$

$$2\pi\sigma_k^2 + \text{Tr}(\mathbf{W}\bar{\mathbf{G}}_{k,i}) \leq e^{y_{k,i}}, \quad 1 \leq i \leq k \leq K, \quad (30c)$$

$$2\pi\sigma_E^2 + \text{Tr}(\mathbf{W}\mathbf{D}_i) \leq e^{y_i}, \quad 1 \leq i \leq K, \quad (30d)$$

Note that constraints (30c) and (30d) are nonconvex, and can be approximated to their corresponding convex forms through the Taylor series expansion; this is similar to (26). Thus, problem (29) can be restricted as follows:

$$\max_{\mathbf{W}, r_s, \{x_{k,i}\}, \{x_i\}, \{y_{k,i}\}, \{y_i\}} r_s \quad (31a)$$

$$s.t. 2^{r_s} e^{y_{k,i} + y_i - x_{k,i} - x_i} \leq 1, \quad 1 \leq i \leq k \leq K, \quad (31b)$$

$$2\pi\sigma_k^2 + \text{Tr}(\mathbf{W}\bar{\mathbf{G}}_{k,i}) \leq e^{\hat{y}_{k,i}} (y_{k,i} - \hat{y}_{k,i} + 1), \quad 1 \leq i \leq k \leq K, \quad (31c)$$

$$2\pi\sigma_E^2 + \text{Tr}(\mathbf{W}\mathbf{D}_i) \leq e^{\hat{y}_i} (y_i - \hat{y}_i + 1), \quad 1 \leq i \leq K,$$

$$(29c), (29d), (29e), (29f), (30a), (30b).$$

Now, problem (31) is quasi-convex, i.e., it is convex for a given $r_s > 0$. Hence, the optimal beamformers of problem (31) can be efficiently obtained using the bisection method. More details on the optimal beamformers of problem (31) can be obtained by solving a sequence of convex feasibility problems with a fixed $r_s > 0$, as follows:

$$\text{find } \{\mathbf{W}, \{x_{k,i}\}, \{x_i\}, \{y_{k,i}\}, \{y_i\}\} \quad (32a)$$

$$s.t. 2^{r_s} e^{y_{k,i} + y_i - x_{k,i} - x_i} \leq 1, \quad 1 \leq i \leq k \leq K, \quad (32b)$$

$$2\pi\sigma_k^2 + \text{Tr}(\mathbf{W}\bar{\mathbf{G}}_{k,i}) \leq e^{\hat{y}_{k,i}} (y_{k,i} - \hat{y}_{k,i} + 1), \quad 1 \leq i \leq k \leq K, \quad (32c)$$

$$2\pi\sigma_E^2 + \text{Tr}(\mathbf{W}\mathbf{D}_i) \leq e^{\hat{y}_i} (y_i - \hat{y}_i + 1), \quad 1 \leq i \leq K,$$

$$(29c), (29d), (29e), (29f), (30a), (30b).$$

Then, we propose a bisection search method to calculate the optimal solutions of problem (32), as shown in Algorithm 1.

Algorithm 1 Bisection Searching Method

- 1) Set upper bound r_l and lower bound r_u such that $r^{\text{opt}} \in [r_l, r_u]$; set tolerance $\varepsilon_e > 0$ and $k = 0$;
- 2) **Repeat**
- 3) $k \leftarrow k + 1$;
- 4) $r_k = \frac{r_l + r_u}{2}$;
- 5) Solve convex problem (32);
- 6) If problem (32) is feasible, set $r_l = r_k$; else, set $r_u = r_k$;
- 7) **Until** if $r_u - r_l \leq \varepsilon_e$, and let $r^{\text{opt}} = r_k$.

V. SIMULATION RESULTS AND DISCUSSION

A. SIMULATION RESULTS OF SECRECY CAPACITY REGION OF NOMA VLC NETWORKS

In this section, we evaluate the proposed outer bound given in (15) and inner bound given in (18) of the secrecy capacity

region. The simulation settings are listed as follows: $K = 2$, $N = 1$, $g_1 = 1$, $g_2 = \frac{1}{2}$, $A \triangleq A_1 = A_2$, $\varepsilon \triangleq \varepsilon_1 = \varepsilon_2$, and $\sigma^2 \triangleq \sigma_1^2 = \sigma_2^2$. Define the amplitude-to-variance ratio as $\varphi \triangleq \frac{A^2}{\varepsilon}$, and define SNR as $SNR \triangleq \frac{\varepsilon}{\sigma^2}$.

Fig. 2 (a)-(c) present the both outer and inner bounds of secrecy channel capacity region of NOMA VLC networks, where $SNR = 10dB$, $\varphi = 6, 8$, and 10 , respectively. In Fig. 2 (a)-(c), we can observe that the inner bound close to the outer bound, and the gap between discrete outer bound and inner bound decreases as the value of φ increases. For the large value $\varphi = 10$, the gap between the outer bound and inner bound approaches zero.

Figs. 3 (a) and (b) depict the sum of the outer and inner bounds of secrecy rates $r_1 + r_2$ (bits/s/Hz) versus SNR (dB), where $\varphi = 6$ and $\varphi = 10$, respectively. Figs. 3 (a) and (b) show that both the outer and inner bounds increase with the SNR. Moreover, the gap between the proposed inner and outer bounds is small at lower SNR, and becomes larger as the SNR increases.

B. SIMULATION RESULTS OF OPTIMAL SECRECY BEAMFORMING DESIGN FOR NOMA VLC NETWORKS

Next, we investigated the of performance of the proposed optimal beamforming design for the total transmit power minimization problem. Consider a typical indoor VLC network scenario, which includes three Bobs ($K = 3$) and one Eve, and the light consists of nine LEDs ($N = 9$). Moreover, we model the room as a three-dimensional coordinate system (X, Y, Z), and one of the room corner is the origin $(0,0,0)$ of the coordinate system. The basic parameters of the VLC system in our simulations are listed in Table 1, and the locations of users and LEDs are listed in Tables 2 and 3, respectively.

TABLE 1. Basic parameters of the VLC system.

LED emission semi-angle	$\phi_{1/2}$	60°
Half of PD's filed-of-view	Ψ_1	90°
Detector area of PD	A_R	$1cm^2$
Current-to-light conversion efficiency	η_c	0.54
Light-to-current conversion efficiency	η_l	1
Average electrical noise power	σ^2	$-98.82dBm$

TABLE 2. Locations of LEDs.

Location		Location	
LED1	$(3, 3, h_{LED})$	LED2	$(3, 5, h_{LED})$
LED3	$(3, 7, h_{LED})$	LED4	$(5, 3, h_{LED})$
LED5	$(5, 5, h_{LED})$	LED6	$(5, 7, h_{LED})$
LED7	$(7, 3, h_{LED})$	LED8	$(7, 5, h_{LED})$
LED9	$(7, 7, h_{LED})$		

TABLE 3. Locations of bobs and eve.

Location		Location	
Bob1	$(9, 9, 1.7)$	Bob2	$(7, 7, 1.7)$
Bob3	$(5, 5, 1.7)$	Eve	$(11, -1, 1.7)$

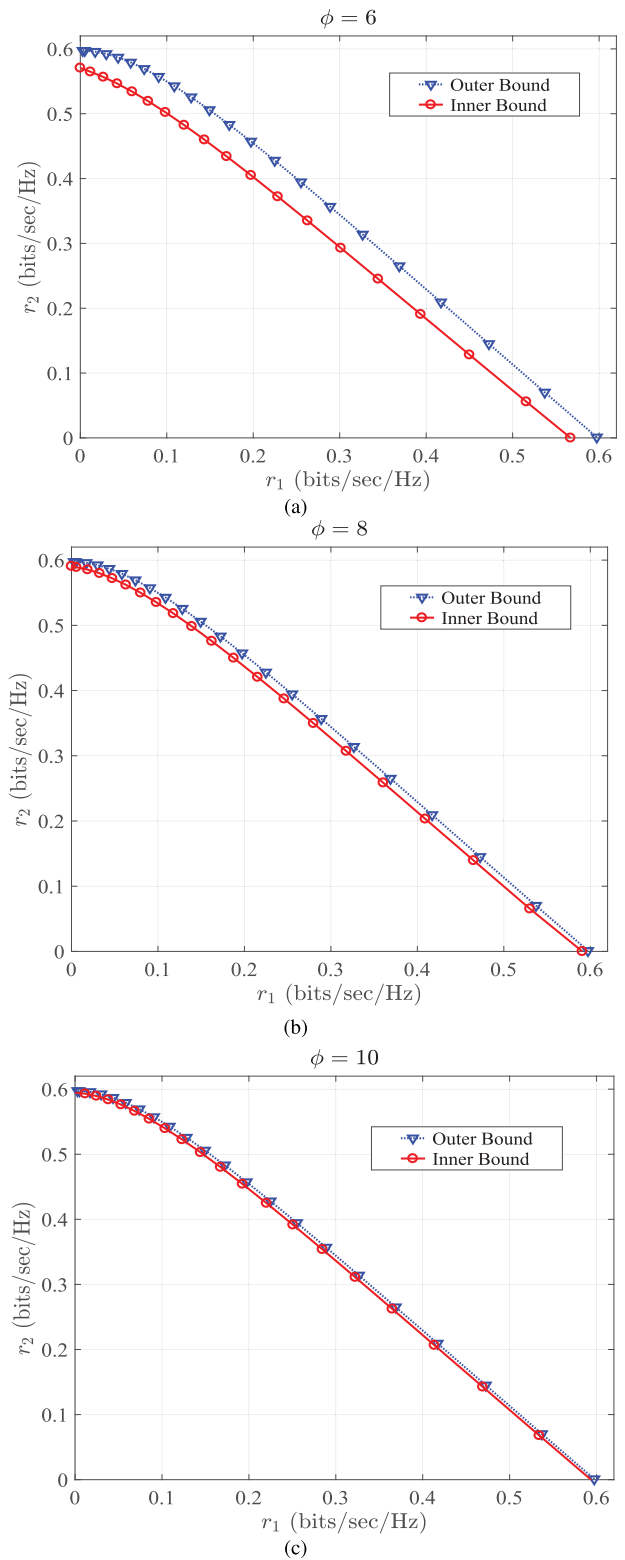


FIGURE 2. Outer and inner bounds of the secrecy capacity region of NOMA VLC networks with (a) $\varphi = 6$, (b) $\varphi = 8$, and (c) $\varphi = 10$.

Fig. 4 (a) shows the total transmit power $\sum_{k=1}^K \varepsilon_k \|\mathbf{w}_k\|^2$ (dBm) versus Bobs' QoS requirements \bar{r} bits/sec/Hz with dimming level $\tau = 0.3, 0.6, 0.9$ and $h_{LED} = 4.5$ (m).

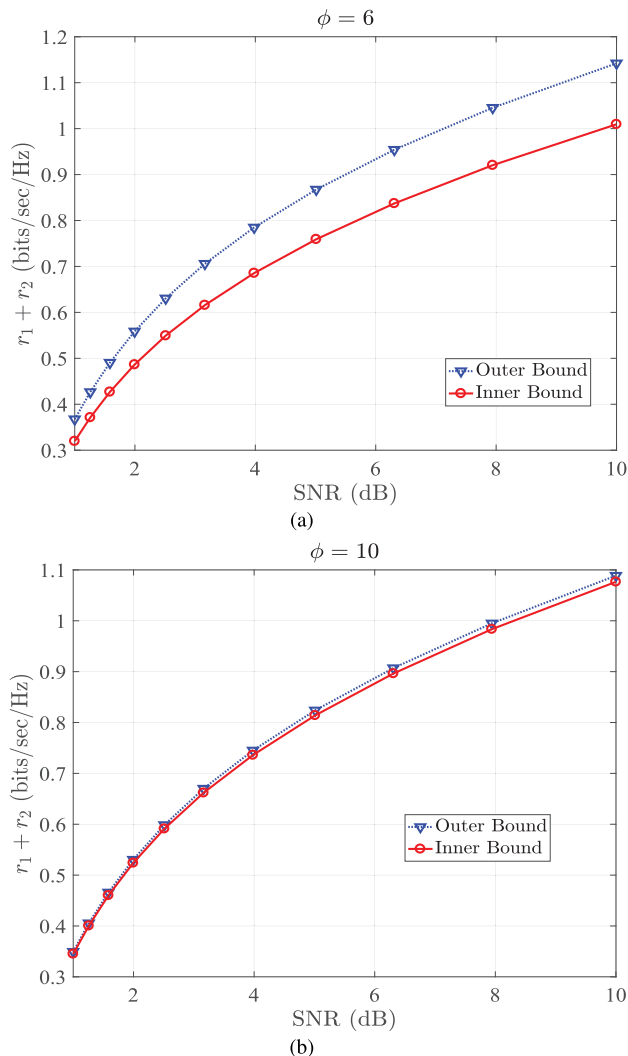


FIGURE 3. The sum secrecy rate of NOMA VLC networks with: (a) $\phi = 6$ and (b) $\phi = 10$.

As shown, the total transmit power increases with the increase in Bobs' QoS requirements under different dimming conditions. Moreover, the total transmit power is almost the same for low QoS requirements, while for high QoS requirements, the total transmit power is inversely proportional to dimming level τ . This is because a higher value of τ will provide a larger feasible region for beamforming design. Fig. 4 (b) shows total transmit power $\sum_{k=1}^K \varepsilon_k \|\mathbf{w}_k\|^2$ (dBm) versus height of the LEDs h_{LED} (m). We observe that as the height of the LEDs increases, the transmit power first decreases, and then increases. This is because that secrecy rate first increases and then decreases as the height of the LEDs increases. Moreover, the higher the Bob's QoS requirements, the more the transmit power is needed.

Finally, Fig. 5 shows minimum secrecy rate $R^{sec} \triangleq \min_{k,i} [R_{k,i}^L - R_{E,i}^U]^+$ versus rate threshold \bar{r} with different power constraints and dimming control levels of

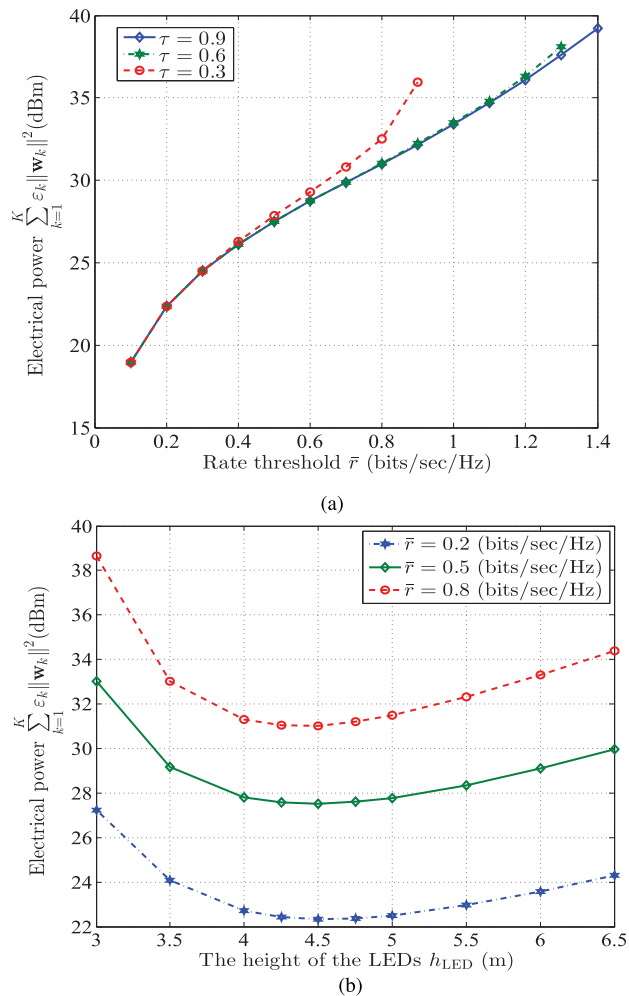


FIGURE 4. Total transmit power $\sum_{k=1}^K \varepsilon_k \|\mathbf{w}_k\|^2$ (dBm) versus (a) Bobs' QoS requirements \bar{r} bits/sec/Hz and (b) the height of the LEDs h_{LED} (m).

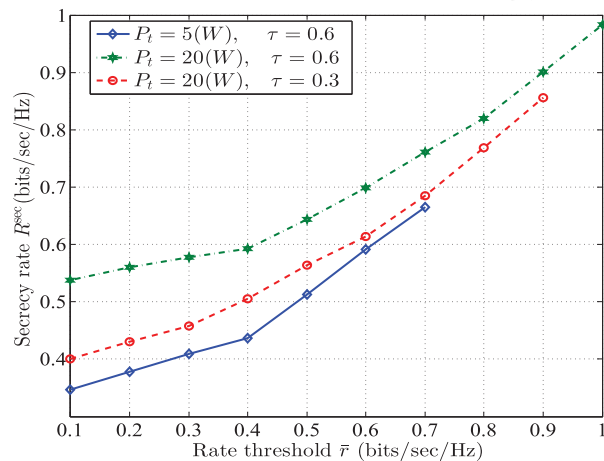


FIGURE 5. Minimum secrecy rate R^{sec} versus rate threshold \bar{r} with different power constraints and dimming control levels: $P_t = 5(W), \tau = 0.6; P_t = 20(W), \tau = 0.6; P_t = 20(W), \tau = 0.3$.

$P_t = 5(W), \tau = 0.6; P_t = 20(W), \tau = 0.6$; and $P_t = 20(W), \tau = 0.3$. Fig. 5 shows that minimum secrecy rate R^{sec} increases as rate threshold \bar{r} increases. Moreover, the comparison of the different power constraints showed

that minimum secrecy rate R^{sec} is larger for higher power constraints. Minimum secrecy rate R^{sec} is also larger for the case of a higher dimming level τ . The reason is that the higher dimming level τ , more power can be used for information transmission.

VI. CONCLUSIONS

This study investigated the security performance of the physical layer when applying the NOMA scheme in VLC networks. Specifically, both the outer and inner bounds of the security capacity region with closed-form expressions were developed. Additionally, we investigated the optimal power allocation problem. For the total transmit power minimization problem, beamformers were designed to minimize the total LED power with dimming control while satisfying both user QoS requirements and secrecy rate constraints. To solve this nonconvex problem, we proposed a relaxation and restriction approach, in which the original nonconvex problem was first relaxed by utilizing the SDR technique, and then was approximated to a convex SDP by using the SCA method. For the minimum secrecy rate maximization problem, beamformers were developed as well under both dimming control and user QoS requirements. By applying the relaxation and restriction approach, the nonconvex problem was reformulated to the quasi-convex form, which could be solved using the bisection search algorithm. The simulation results verified that the proposed beamforming design schemes can guarantee both the security and QoS requirements of NOMA VLC networks.

REFERENCES

- [1] J. G. Andrews et al., "What will 5G be?" *IEEE J. Sel. Areas Commun.*, vol. 32, no. 6, pp. 1065–1082, Jun. 2014.
- [2] V. Chandrasekhar, J. G. Andrews, and A. Gatherer, "Femtocell networks: A survey," *IEEE Commun. Mag.*, vol. 46, no. 9, pp. 59–67, Sep. 2008.
- [3] Z. Pi and F. Khan, "An introduction to millimeter-wave mobile broadband systems," *IEEE Commun. Mag.*, vol. 49, no. 6, pp. 101–107, Jun. 2011.
- [4] S. Rangan, T. S. Rappaport, and E. Erkip, "Millimeter-wave cellular wireless networks: Potentials and challenges," *Proc. IEEE*, vol. 102, no. 3, pp. 366–385, Mar. 2014.
- [5] T. Komine and M. Nakagawa, "Fundamental analysis for visible-light communication system using LED lights," *IEEE Trans. Consum. Electron.*, vol. 50, no. 1, pp. 100–107, Feb. 2004.
- [6] H. Elgala, R. Mesleh, and H. Haas, "Indoor optical wireless communication: Potential and state-of-the-art," *IEEE Commun. Mag.*, vol. 49, no. 9, pp. 56–62, Sep. 2011.
- [7] S. Arnon, J. Barry, G. Karagiannidis, R. Schober, and M. Uysal, *Advanced Optical Wireless Communication Systems*, 1st ed. Cambridge, U.K.: Cambridge Univ. Press, 2012.
- [8] A. Jovicic, J. Li, and T. Richardson, "Visible light communication: Opportunities, challenges and the path to market," *IEEE Commun. Mag.*, vol. 51, no. 12, pp. 26–32, Dec. 2013.
- [9] P. H. Pathak, X. Feng, P. Hu, and P. Mohapatra, "Visible light communication, networking, and sensing: A survey, potential and challenges," *IEEE Commun. Surveys Tuts.*, vol. 17, no. 4, pp. 2047–2077, 4th Quart., 2015.
- [10] Z. Ding, X. Lei, G. K. Karagiannidis, R. Schober, J. Yuan, and V. Bhargava, "A survey on non-orthogonal multiple access for 5G networks: Research challenges and future trends," *IEEE J. Sel. Areas Commun.*, vol. 35, no. 10, pp. 2181–2195, Oct. 2017.
- [11] Q. Li, M. Wen, E. Basar, H. V. Poor, and F. Chen, "Spatial modulation-aided cooperative NOMA: Performance analysis and comparative study," *IEEE J. Sel. Topics Signal Process.*, to be published.
- [12] B. Zheng et al., "Secure NOMA based two-way relay networks using artificial noise and full duplex," *IEEE J. Sel. Areas Commun.*, vol. 36, no. 7, pp. 1426–1440, Jul. 2018.
- [13] D. Wan, M. Wen, F. Ji, H. Yu, and F. Chen, "Non-orthogonal multiple access for cooperative communications: Challenges, opportunities, and trends," *IEEE Wireless Commun.*, vol. 25, no. 2, pp. 109–117, Apr. 2018.
- [14] L. Dai, B. Wang, Y. Yuan, S. Han, C.-L. I, and Z. Wang, "Non-orthogonal multiple access for 5G: Solutions, challenges, opportunities, and future research trends," *IEEE Commun. Mag.*, vol. 53, no. 9, pp. 74–81, Sep. 2015.
- [15] D. Wan, M. Wen, F. Ji, Y. Liu, and Y. Huang, "Cooperative NOMA systems with partial channel state information over Nakagami- m fading channels," *IEEE Trans. Commun.*, vol. 66, no. 3, pp. 947–958, Mar. 2018.
- [16] M. Xu, F. Ji, M. Wen, and W. Duan, "Novel receiver design for the cooperative relaying system with non-orthogonal multiple access," *IEEE Commun. Lett.*, vol. 20, no. 8, pp. 1679–1682, Aug. 2016.
- [17] B. Zheng, X. Wang, M. Wen, and F. Chen, "NOMA-based multi-pair two-way relay networks with rate splitting and group decoding," *IEEE J. Sel. Areas Commun.*, vol. 35, no. 10, pp. 2328–2341, Oct. 2017.
- [18] Z. Ding, Z. Yang, P. Fan, and H. V. Poor, "On the performance of non-orthogonal multiple access in 5G systems with randomly deployed users," *IEEE Signal Process. Lett.*, vol. 21, no. 12, pp. 1501–1505, Dec. 2014.
- [19] T. Fath and H. Haas, "Performance comparison of MIMO techniques for optical wireless communications in indoor environment," *IEEE Trans. Commun.*, vol. 61, no. 2, pp. 733–742, Feb. 2013.
- [20] S. Ma, Z.-L. Dong, H. Li, Z. Lu, and S. Li, "Optimal and robust secure beamformer for indoor MISO visible light communication," *J. Lightw. Technol.*, vol. 34, no. 21, pp. 4988–4998, Nov. 1, 2016.
- [21] A. D. Wyner, "The wire-tap channel," *Bell Syst. Tech. J.*, vol. 54, no. 8, pp. 1355–1387, Oct. 1975.
- [22] Z. Li, W. Trappe, and R. Yates, "Secret communication via multi-antenna transmission," in *Proc. 41st Annu. Conf. Inf. Sci. Syst. (CISS)*, Mar. 2007, pp. 905–910.
- [23] Y. Liang, H. V. Poor, and S. S. Shamai, "Information theoretic security," *Found. Trends Commun. Inf. Theory*, vol. 5, nos. 4–5, pp. 355–380, Apr. 2009.
- [24] S. Ma, M. Hong, E. Song, X. Wang, and D. Sun, "Outage constrained robust secure transmission for MISO wiretap channels," *IEEE Trans. Wireless Commun.*, vol. 13, no. 10, pp. 5558–5570, Oct. 2014.
- [25] Y. Zhang, H.-M. Wang, Q. Yang, and Z. Ding, "Secrecy sum rate maximization in non-orthogonal multiple access," *IEEE Commun. Lett.*, vol. 20, no. 5, pp. 930–933, May 2016.
- [26] Y. Li, M. Jiang, Q. Zhang, Q. Li, and J. Qin, "Secure beamforming in downlink MISO nonorthogonal multiple access systems," *IEEE Trans. Veh. Technol.*, vol. 66, no. 8, pp. 7563–7567, Aug. 2017.
- [27] M. Tian, Q. Zhang, S. Zhao, Q. Li, and J. Qin, "Secrecy sum rate optimization for downlink MIMO nonorthogonal multiple access systems," *IEEE Signal Process. Lett.*, vol. 24, no. 8, pp. 1113–1117, Aug. 2017.
- [28] M. Jiang, Y. Li, Q. Zhang, Q. Li, and J. Qin, "Secure beamforming in downlink MIMO nonorthogonal multiple access networks," *IEEE Signal Process. Lett.*, vol. 24, no. 12, pp. 1852–1856, Dec. 2017.
- [29] Y. Liu, Z. Qin, M. El-kashlan, Y. Gao, and L. Hanzo, "Enhancing the physical layer security of non-orthogonal multiple access in large-scale networks," *IEEE Trans. Wireless Commun.*, vol. 16, no. 3, pp. 1656–1672, Mar. 2017.
- [30] B. He, A. Liu, N. Yang, and V. K. N. Lau, "On the design of secure non-orthogonal multiple access systems," *IEEE J. Sel. Areas Commun.*, vol. 35, no. 10, pp. 2196–2206, Oct. 2017.
- [31] H. Lei et al., "On secure NOMA systems with transmit antenna selection schemes," *IEEE Access*, vol. 5, pp. 17450–17464, 2017.
- [32] X. Zhao, H. Chen, and J. Sun, "On physical-layer security in multiuser visible light communication systems with non-orthogonal multiple access," *IEEE Access*, vol. 6, pp. 34004–34017, 2018.
- [33] Z. Ding, Z. Zhao, M. Peng, and H. V. Poor, "On the spectral efficiency and security enhancements of NOMA assisted multicast-unicast streaming," *IEEE Trans. Commun.*, vol. 65, no. 7, pp. 3151–3163, Jul. 2017.
- [34] S. Rajagopal, R. D. Roberts, and S.-K. Lim, "IEEE 802.15.7 visible light communication: Modulation schemes and dimming support," *IEEE Commun. Mag.*, vol. 50, no. 3, pp. 72–82, Mar. 2012.
- [35] T. M. Cover and J. A. Thomas, *Elements of Information Theory*, 2nd ed. New York, NY, USA: Wiley, 2006.
- [36] Q. Gao, C. Gong, and Z. Xu, "Joint transceiver and offset design for visible light communications with input-dependent shot noise," *IEEE Trans. Wireless Commun.*, vol. 16, no. 5, pp. 2736–2747, May 2017.
- [37] J. M. Kahn and J. R. Barry, "Wireless infrared communications," *Proc. IEEE*, vol. 85, no. 2, pp. 265–298, Feb. 1997.

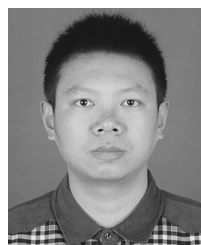
- [38] T. Q. Wang, Y. A. Sekercioglu, and J. Armstrong, "Analysis of an optical wireless receiver using a hemispherical lens with application in MIMO visible light communications," *J. Lightw. Technol.*, vol. 31, no. 11, pp. 1744–1754, Jun. 1, 2013.
- [39] I. Csiszar and J. Korner, "Broadcast channels with confidential messages," *IEEE Trans. Inf. Theory*, vol. IT-24, no. 3, pp. 339–348, May 1978.
- [40] J. G. Smith, "The information capacity of amplitude- and variance-constrained scalar gaussian channels," *Inf. Control*, vol. 18, no. 3, pp. 203–219, Apr. 1971.
- [41] S. Ma, Y. He, H. Li, S. Lu, F. Zhang, and S. Li, "Optimal power allocation for mobile users in non-orthogonal multiple access visible light communication network," *IEEE Trans. Commun.*, vol. 67, no. 3, pp. 2233–2244, Mar. 2019.
- [42] S. Ma *et al.*, "Capacity bounds and interference management for interference channel in visible light communication networks," *IEEE Trans. Wireless Commun.*, vol. 18, no. 1, pp. 182–193, Jan. 2019.
- [43] S. Boyd and L. Vandenberghe, *Convex Optimization*. Cambridge, U.K.: Cambridge Univ. Press, 2004.
- [44] W.-C. Li, T.-H. Chang, C. Lin, and C.-Y. Chi, "Coordinated beamforming for multiuser MISO interference channel under rate outage constraints," *IEEE Trans. Signal Process.*, vol. 61, no. 5, pp. 1087–1103, Mar. 2013.



CHUN DU received the B.S. degree from the China University of Mining and Technology, Xuzhou, China, in 2011, and the M.E. degree from Duisburg-Essen University, Westfalen, Germany, in 2014. He is currently pursuing the Ph.D. degree in information and communication engineering with the School of Information and Control Engineering, China University of Mining and Technology. His research interests include visible light communication, wireless communications, and physical layer security.

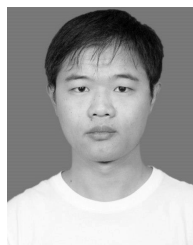


FAN ZHANG received the B.S. degree from the China University of Mining and Technology, Xuzhou, China, in 2018, where she is currently pursuing the M.E. degree in information and communication engineering with the School of Information and Control Engineering. Her research interests include visible light communication, wireless communications, and network information theory.



interests include visible light communication, machine learning, wireless communications, and network information theory.

SHUAI MA received the B.S. and Ph.D. degrees in communication and information systems from Xidian University, Xi'an, China, in 2009 and 2016, respectively. From 2014 to 2015, he was a Visiting Scholar with the Department of Electrical and Computer Engineering, Texas A&M University, College Station, TX, USA. Since 2019, he has been an Associate Professor with the School of Information and Control Engineering, China University of Mining and Technology. His research



YIXIAO TANG received the B.S. degree from Northwestern Polytechnical University, Xi'an, China, in 2018. He is currently pursuing the M.E. degree in information and communication engineering with the School of Information and Control Engineering, China University of Mining and Technology, Xuzhou, China. His research interests include visible light communication, wireless communications, and network information theory.



His current research interests include wireless networks, stochastic optimization, and the applications of machine learning.

HANG LI (S'13–M'16) received the B.E. and M.S. degrees from Beihang University, Beijing, China, in 2008 and 2011, respectively, and the Ph.D. degree from Texas A&M University, College Station, TX, USA, in 2016, where he was a Postdoctoral Research Associate, from 2016 to 2017 and also with the University of California at Davis, from 2017 to 2018. Since 2018, he has been a Visiting Research Scholar with the Shenzhen Research Institute of Big Data, Shenzhen, China.



HONGMEI WANG received the Ph.D. degree from the School of Mechatronics Engineering, Changwon National University, South Korea, in 2012. She is currently a Lecturer with the School of Information and Control Engineering, China University of Mining and Technology. Her research interests include designing system applied for wireless communication modem and various system required advanced digital signal processing.



SHIYIN LI received the Ph.D. degree in information and communication engineering from the China University of Mining and Technology, Xuzhou, China, in 2010, where he has been a Professor with the School of Information and Control Engineering, since 2010. He is currently the Head of the Department of Information Engineering. His research interests include wireless communication and network congestion control.

...